Appl Phys A (2009) 96: 363–367
DOI 10.1007/s00339-009-5196-0

Applied Physics A
Materials Science & Processing

Dielectric function dynamics during femtosecond laser excitation of bulk ZnO

T. Shih · M.T. Winkler · T. Voss · E. Mazur

Received: 8 December 2008 / Accepted: 3 March 2009 / Published online: 25 March 2009

Abstract Using a broad band dual-angle pump-probe reflectometry technique, we obtained the ultrafast dielectric function dynamics of bulk ZnO under femtosecond laser excitation. We determined that multiphoton absorption of the 800-nm femtosecond laser excitation creates a large population of excited carriers with excess energy. Screening of the Coulomb interaction by the excited free carriers causes damping of the exciton resonance and renormalization of the band gap causing broadband (2.3–3.5 eV) changes in the dielectric function of ZnO. From the dielectric function, many transient material properties, such as the index of refraction of ZnO under excitation, can be determined to optimize ZnO-based devices.

PACS 81.05.Dz · 78.47.J

1 Introduction

Zinc oxide (ZnO) is a wide-band-gap semiconductor that has recently gained renewed interest as an ideal material system for the development of optoelectronic devices and lasing media in the blue-to-near-UV spectral region [1, 2]. Known for its large band gap and large exciton binding energy [2, 3], ZnO can easily be handled to yield uniform and high-quality ZnO nanostructures and its fabrication does not require toxic precursors [4–6]. In order to better understand ZnO and its relevant properties for optoelectronic applications, it is necessary to know the carrier dynamics in ZnO after excitation with intense ultrafast laser pulses.

Under intense ultrafast excitation, semiconductors undergo dramatic changes because the induced high carrier density can cause heating, melting, ablation, and resolidification, which permanently modify the morphology of the material [7–10]. Figure 1 shows an example of the permanent surface modification in ZnO after exposure to high-intensity ultrashort laser pulses. While typical ZnO-based applications do not require permanent changes in the material, most applications involve a large population of excited carriers. The performance of lasers and waveguides, for example, depend strongly on the carrier density and other material properties. It is therefore necessary to understand how ZnO behaves under high carrier densities over time in order to optimize ZnO-based devices. While the nonlinear optical properties of ZnO under ultrashort laser irradiation have been investigated [11–13], there are no studies on the related timescales and broadband dynamics of the large population of excited carriers in ZnO after ultrafast laser excitation. Characterization of ZnO under high-excitation conditions not only provides additional information on the excitation, thermalization, scattering, and recombination of the carriers, but also reveals how high carrier densities affect the dielectric function of ZnO.

In this paper, we perform systematic time and energy resolved pump-probe studies that yield the time-resolved ZnO dielectric function after excitation with femtosecond laser pulses [14]. The data suggests that excitation with femtosecond laser pulses of sub-band-gap photon energy creates a large number of free carriers. The generated free carriers

T. Shih (✉) · M.T. Winkler · T. Voss · E. Mazur
Department of Physics and School of Engineering and Applied Sciences, Harvard University, 9 Oxford Street, Cambridge, MA 02138, USA
e-mail: tinashih@fas.harvard.edu

T. Voss
Institute of Solid-State Physics, University of Bremen, Bremen, Germany

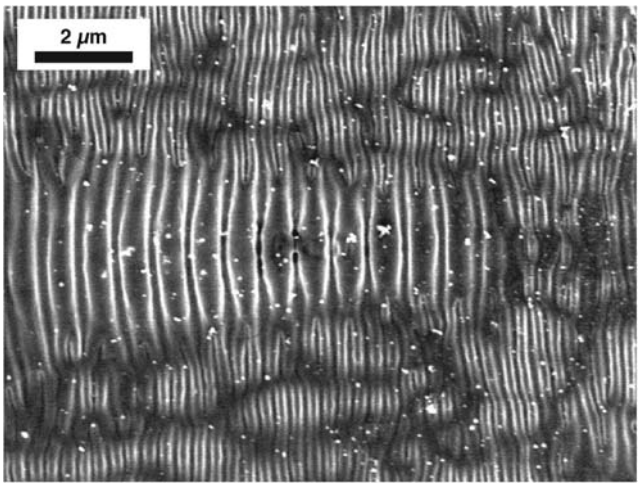

Fig. 1 SEM image of femtosecond laser-structured bulk ZnO

cause screening of the Coulomb interaction which subsequently damps the exciton resonance and renormalizes the band gap causing broad band (2.3–3.5 eV) changes in the dielectric function of ZnO. Information about the dielectric function yields a number of pertinent material properties of ZnO, including the change in the index of refraction as a function of time after fs laser excitation. The measurement of the dielectric function and the index of refraction during and after intense excitation enables a better understanding of the carrier dynamics in highly excited ZnO, which in turn will permit optimizing the design of ZnO-based devices [15–19].

2 Experimental details

We performed dual-angle-of-incidence pump-probe spectroscopy to measure the changes in the reflectivity and invert the data into the transient dielectric function [14] of ZnO under ultrafast laser excitation. Using a multipass amplified Ti:sapphire laser (0.5-mJ pulse energy, 40-fs pulse width, 1-kHz repetition rate), we excite the *c*-plane of a crystalline ZnO sample under normal atmosphere and room temperature conditions. The pump pulse, centered at 800 nm, had a fluence of 2.5 kJ/m^2, just below the ZnO damage threshold of 3.0 kJ/m^2. The excitation fluence used to obtain reflectivity and dielectric function dynamics is different from the above-damage-threshold excitation fluence of 4.0 kJ/m^2 used to laser structure the surface of bulk ZnO (Fig. 1). Focusing the laser pulse through a CaF_2 crystal, we generate a broadband (1.5–3.5 eV) probe pulse to detect reflectivity changes of the excited ZnO at different pump-probe delay times. Using the reflectivity data measurements taken at multiple angles of incidence, we reconstruct the time-resolved dielectric function of the highly excited ZnO [14].

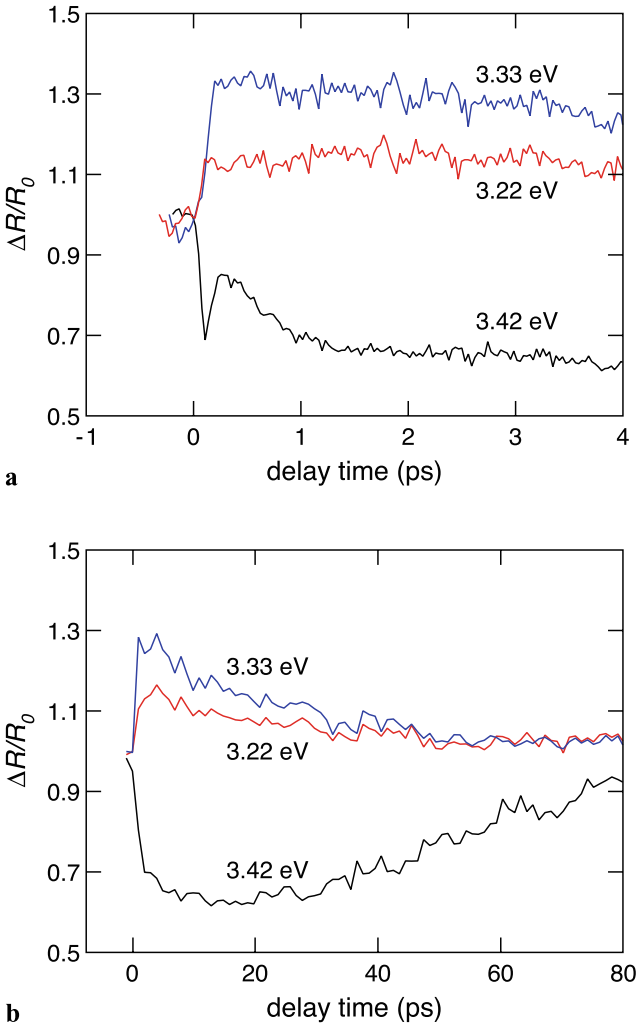

Fig. 2 Ultrafast reflectivity of bulk ZnO for an excitation fluence of 2.5 kJ/m^2 at three different photon energy ranges: above band gap energy 3.42 eV (*black*); at the exciton resonance energy 3.33 eV (*blue*); and below the band gap energy—3.25 eV. Reflectivity is plotted as a function of pump-probe delay time (**a**) from −1 to 4 ps in steps of 33 fs and (**b**) from −2 to 80 ps in steps of 1 ps

3 Results

We measured the ultrafast reflectivity response at photon energies from 1.5 to 3.5 eV for an excitation fluence of 2.5 kJ/m^2. Figure 2a shows the reflectivity data as a function of delay time (0–4 ps) at three characteristic photon energy ranges: below the band gap at 3.25 eV (red line), at the exciton resonance of 3.32 eV (blue line), and above the band gap at 3.42 eV (black line). For all three energies, the reflectivity data show a fast response over several hundred femtoseconds followed by a slower decay back towards equilibrium over several tens of picoseconds. Below the band-gap energy, the reflectivity takes 200 fs to increase by 15% and then decays after 3 ps. At the exciton resonance, the reflectivity sharply increases by 40% over 200 fs and decays

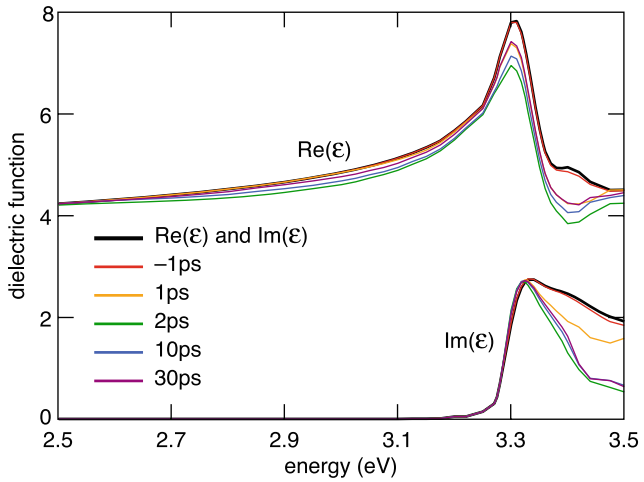

Fig. 3 Dielectric function of ZnO as a function of energy (2.5–3.5 eV) for various pump-probe delay times after excitation from

immediately thereafter. Above the band-gap energy, the reflectivity sharply decreases by 30% within 150 fs, recovers halfway after 250 fs, and then continues to decrease on a longer timescale. Figure 2b depicts the reflectivity dynamics over a longer time window (−2 to 80 ps) and shows that the reflectivity for energies above the band gap starts to increase back towards unexcited ZnO reflectivities after 20 ps. In addition, complete recovery occurs within 150 ps for all photon energies thus indicating that the measurements are below the damage threshold and can be repeated.

From the dual-angle broadband reflectivity measurements we can extract the time-resolved dielectric function of the highly excited ZnO [14]. Figure 3 shows the resulting real and imaginary components of the dielectric function of ZnO at different pump-probe delay times. For reference, the black line represents the linear dielectric function of the sample, as measured using ellipsometry. The ultrafast dynamics of the dielectric function is plotted for different delay times ranging from −1 to 30 ps after excitation. For energies above the band gap, the real and imaginary parts of the dielectric function decrease by 25% within the first few hundred femtoseconds. Excitation effects can be seen for delay times well beyond a few picoseconds and for photon energies far below 3 eV. In particular, a decrease in the real part of the dielectric function stretches from 3.5 eV down to at least 2.5 eV. Near the exciton resonance (3.31 eV) the real part shows a 25% decrease of the resonance from 7.8 to 6.9 as well as a large decrease from 4.9 to 3.8 at 3.4 eV. The imaginary part shows an initial decrease from 2.2 to 0.7 at energies above resonance, followed by a recovery after 2 ps. The data also show a redshift of the maximum of the imaginary part of about 15–20 meV.

4 Discussion

Because the pump photon energy (1.55 eV) is well below 3.35 eV, the room-temperature band gap of ZnO, multiphoton processes are required to induce interband transitions. We measured the ZnO photoluminescence and found the multiphoton process to have a higher contribution from two-photon absorption than three-photon absorption, even though the energy of two photons is not quite enough to bridge the band gap. This finding is in agreement with reports in literature, because the cross section of two-photon absorption is much larger than that of three-photon absorption [11], most likely due to electric-field-assisted two-photon absorption caused by the high electric fields in the amplified femtosecond laser pulses [20]. Evidence of multiphoton absorption can also be seen in the periodic structures on the surface of ZnO, generated by 800-nm above-damage-threshold laser excitation (Fig. 1). These features, which are often observed on material surfaces upon exposure to short pulse irradiation, have a spacing of λ or λ/n, where λ is the incident laser wavelength and n is an integer [21, 22]. During femtosecond laser structuring of ZnO, we observe emission at $\lambda = 800$ and 400 nm indicating that second-harmonic generation, a common phenomenon upon ultrafast excitation of a highly polar semiconductor like ZnO [23], occurs at the surface. The presence of ZnO surface feature sizes that correspond to these wavelengths indicates that the absorption causing the structuring must be nonlinear.

The reflectivity measurements in Fig. 2 reveal three timescales in the dynamics of photoexcited ZnO. The first timescale is the fast initial 200-fs reflectivity change resulting from multiphoton absorption of the incident 800-nm pulses. Multiphoton absorption creates a large number of highly excited electron–hole pairs that occupy states well above the conduction band edge. Above the band gap, at 3.42 eV, the reflectivity shows temporary decrease on this timescale, which we attribute to pump-induced nonlinear absorption [12, 24]. Around zero time delay in pump-probe spectroscopy studies, a pump photon may have the opportunity to interact with one or more probe photons inducing a nonlinear absorption and creating a large reflectivity decrease that disappears after about two pulse widths in time [12, 24].

The second timescale is on the order of 1 ps and is associated with the time required for the hot carriers to reach a quasithermal equilibrium [25]. This 1-ps timescale is most visible for the above band gap energy reflectivities (Fig. 2a, black line) because this energy range probes the hot carriers that relaxing down to states near the exciton resonance.

About 20 ps after excitation a third timescale emerges in the reflectivity data (Fig. 2b). Starting at about 20 ps the reflectivity gradually reverts to the value for unexcited ZnO.

Indeed, this timescale correlates well with recombination timescales obtained from photoluminescence measurements in ZnO [26]. The reflectivity completely returns to the reflectivity of unexcited ZnO in about 150 ps. The 150-ps timescale agrees with previous work, which reports a carrier recombination time in ZnO of about 100–300 ps [27, 28].

The dielectric function of ZnO shown in Fig. 3 provides additional detail on the interaction of ultrafast laser excitation with ZnO revealing how multiphoton absorption of the pump affects the carriers, how excited carriers affect the exciton resonance, and how excitation affects the material response. The femtosecond laser excitation creates a large concentration of free electron–hole pairs via multiphoton absorption of 800-nm photons. The initial decrease in both the real and imaginary components of the dielectric function above 3.35 eV is indicative of an increase of carrier concentration at energies above the conduction band minimum. The high density of free electron–hole pairs significantly screen the Coulomb interaction and damp the exciton resonance, as evidenced by the 20% decrease of the real part of the dielectric function at 3.33 eV in Fig. 3. Immediately after excitation, the imaginary part near 3.33 eV shows a small 20-meV redshift which we can attribute to a reduction of the band gap due to Coulomb screening [19, 20]. At time delays of 1–2 ps the carriers have thermalized, and over tens of picoseconds the carrier relax through LO phonons [12] restoring the dielectric function to that of unexcited ZnO.

The dielectric function data can be used to obtain the transient behavior of other material properties, such as the index of refraction. Knowing how the index of refraction is affected by high carrier concentrations is important for modeling and designing ZnO devices. Previous studies on ultrafast laser excitation of ZnO waveguides [18, 29] and ZnO-based lasers [16, 19] revealed an unexpected blueshift of the waveguide or cavity modes relative to calculated models. These unexpected mode changes may be due to a change in the index of refraction of ZnO induced by the laser excitation. From the dielectric function data, we see that the changes in the real part are largest (about 20%) near the band gap (3.33 eV) which implies that there is also a large change in the index of refraction near the band gap.

5 Conclusion

In summary, we measured the dielectric function dynamics of bulk ZnO under femtosecond laser excitation by performing broadband dual-angle pump-probe reflectometry. We find that sub-band-gap below-damage-threshold excitation creates excited electron–hole pairs in ZnO by way of multiphoton absorption. The large population of excited carriers generated from ultrafast laser excitation cause screening of the Coulomb interaction which subsequently damps the exciton resonance and renormalizes the band gap. These changes contribute to broadband changes in the dielectric function of ZnO from 2.5 to 3.5 eV. The observed dynamics in the dielectric function sheds light on how the index of refraction of ZnO changes under ultrafast excitation.

Acknowledgements Several people contributed to the work described in this paper. T.V. conceived of the basic idea for this work. M.W., T.S., T.V. designed and carried out the experiments and analyzed the results. E.M. supervised the research and the development of the manuscript. This work was carried out with the financial support of the National Science Foundation under contract DMI-0334984 and the Army Research Office under contract W911NF-05-1-0471. T.S. and M.W. would like to acknowledge support from NSF Graduate Research Fellowship, and T.V. acknowledges support from the German Research Foundation (DFG) under contract VO1265/3.

References

1. C. Klingshirn, R. Hauschild, H. Priller, M. Decker, J. Zeller, H. Kalt, Superlattices Microstruct. **38**, 209 (2005)
2. D.C. Look, Mater. Sci. Eng. B-Solid State Mater. Adv. Technol. **80**, 383 (2001)
3. H. Yoshikawa, S. Adachi, Jpn. J. Appl. Phys. Part 1-Regul. Pap. Short Notes Rev. Pap. **36**, 6237 (1997)
4. C. Borchers, S. Muller, D. Stichtenoth, D. Schwen, C. Ronning, J. Phys. Chem. B **110**, 1656 (2006)
5. Y. Huang, X.F. Duan, C.M. Lieber, Small **1**, 142 (2005)
6. P.J. Pauzauskie, P. Yang, Mater. Today **9**, 36 (2006)
7. A. Cavalleri, C. Toth, C.W. Siders, J.A. Squier, F. Raksi, P. Forget, J.C. Kieffer, Phys. Rev. Lett. **87**, 401 (2001)
8. C. Guo, G. Rodriguez, A. Lobad, A.J. Taylor, Phys. Rev. Lett. **84**, 4493 (2000)
9. P.N. Saeta, J.K. Wang, Y. Siegal, N. Bloembergen, E. Mazur, Phys. Rev. Lett. **67**, 1023 (1991)
10. K. Sokolowski-Tinten, J. Solis, J. Bialkowski, J. Siegel, C.N. Alfonso, D.v.d. Linde, Phys. Rev. Lett. **81**, 3679 (1998)
11. D.C. Dai, S.J. Xu, S.L. Shi, M.H. Xie, C.M. Che, Opt. Lett. **30**, 3377 (2005)
12. C.K. Sun, S.Z. Sun, K.H. Lin, K.Y.J. Zhang, H.L. Liu, S.C. Liu, J.J. Wu, Appl. Phys. Lett. **87** (2005)
13. X.J. Zhang, W. Ji, S.H. Tang, J. Opt. Soc. Am. B-Opt. Phys. **14**, 1951 (1997)
14. C.A.D. Roeser, A.M.T. Kim, J.P. Callan, L. Huang, E.N. Glezer, Y. Siegal, E. Mazur, Rev. Sci. Instrum. **74**, 3413 (2003)
15. J.M. Bao, M.A. Zimmler, F. Capasso, X.W. Wang, Z.F. Ren, Nano Lett. **6**, 1719 (2006)
16. A.B. Djurisic, W.M. Kwok, Y.H. Leung, W.K. Chan, D.L. Phillips, M.S. Lin, S. Gwo, Nanotechnology **17**, 244 (2006)
17. R. Hauschild, H. Lange, H. Priller, C. Klingshirn, R. Kling, A. Waag, H.J. Fan, M. Zacharias, H. Kalt, Phys. Status Solidi B-Basic Solid State Phys. **243**, 853 (2006)
18. J.C. Johnson, H.Q. Yan, P.D. Yang, R.J. Saykally, J. Phys. Chem. B **107**, 8816 (2003)
19. J.K. Song, J.M. Szarko, S.R. Leone, S.H. Li, Y.P. Zhao, J. Phys. Chem. B **109**, 15749 (2005)
20. Z.W. Dong, C.F. Zhang, G.J. You, X.Q. Qiu, K.J. Liu, Y.L. Yan, S.X. Qian, J. Phys.-Condens. Matter **19** (2007)
21. J.E. Sipe, J.F. Young, J.S. Preston, H.M.v. Driel, Phys. Rev. B **27**, 1141 (1983)
22. J.E. Young, J.S. Preston, H.M.v. Driel, J.E. Sipe, Phys. Rev. B **27**, 1155 (1983)

23. U. Neumann, R. Grunwald, U. Griebner, G. Steinmeyer, W. Seeber, Appl. Phys. Lett. **84**, 170 (2004)
24. K.H. Lin, G.W. Chern, Y.C. Huang, S. Keller, S.P. DenBaars, C.K. Sun, Appl. Phys. Lett. **83**, 3087 (2003)
25. A. Yamamoto, T. Kido, Y.F. Goto, Y. Chen, T. Yao, A. Kasuya, Appl. Phys. Lett. **75**, 469 (1999)
26. T. Voss, L. Wischmeier, J. Nanosci. Nanotechnol. **8**, 228 (2008)
27. J.C. Johnson, K.P. Knutsen, H.Q. Yan, M. Law, Y.F. Zhang, P.D. Yang, R.J. Saykally, Nano Lett. **4**, 197 (2004)
28. D.C. Reynolds, D.C. Look, B. Jogai, J.E. Hoelscher, R.E. Sherriff, M.T. Harris, M.J. Callahan, J. Appl. Phys. **88**, 2152 (2000)
29. R. Hauschild, H. Kalt, Appl. Phys. Lett. **89** (2006)